AFCRL-68-0027

NETWORK THEORY PROBLEMS IN IMPEDANCE LOADING

by

E. Lawrence McMahon, Arthur R. Braun,
Raymond S. Kasevich
The University of Michigan
Radiation Laboratory
201 Catherine Street
Ann Arbor, Michigan 48108

January 1968

Scientific Report No. 8

Contract AF 19(628)-2374
Project 5635
Task 563502
Work Unit No. 56350201

Contract Monitor: Philipp Blacksmith
Microwave Physics Laboratory

Prepared for

Air Force Cambridge Research Laboratories
Office of Aerospace Research
L.G. Hanscom Field
Bedford, Massachusetts

ABSTRACT

Relationships between the real and imaginary parts of an impedance are studied. Given the real and imaginary parts in a finite frequency band, a technique is developed for finding these parts outside the band. Conditions under which the real part remains positive for all ω are given.

Use of a negative impedance converter for realization of a particular impedance arising from impedance loading studies is discussed. A method of compensating for collector capacitance and extending operation of a transistorized NIC into the VHF region is given.

TABLE OF CONTENTS

I

INTRODUCTION

This report is devoted to those aspects of the impedance loading problem which are concerned with network theory rather than with field theory.

In seeking to control the radar cross-section of a conducting body by impedance loading, the scattering behavior of the body is first determined as a function of loading impedance, either lumped (as for a thin wire) or distributed (as, for example, with a sphere). The equations are then solved to give the impedance, as a function of frequency, necessary to obtain the desired cross-section modification. The network-theory problem is that of synthesizing and realizing this impedance from numerical data giving its real and imaginary parts over some band of frequencies.

Network synthesis actually involves two separate problems, approximation and realization. The given data must first be approximated by a rational function of frequency chosen from an appropriate class of rational functions (e.g., positive-real functions). A network realizing this rational function is then obtained by any of several fairly standard techniques.

The approximation problem arising from the impedance-loading study is a rather unusual one. Both the real and imaginary parts of the impedance are specified over some relatively large, but finite, band of frequencies; the more common situation is for some one quantity, such as magnitude, to be specified over the entire frequency range.

The unusual nature of the problem has prompted a theoretical study of the relations between parts of impedances specified over a finite band. A number of interesting and useful results have been obtained, and are reported in the next sections. These results are expected to form the basis for techniques of handling a large class of network problems arising in connection with reactive loading.

An experimental program, aimed at more immediate practical results in a specific case, has also been undertaken. This program has attempted to obtain an active-network realization of an impedance whose behavior is approximated by a pure negative reactance; such an impedance was found by Chang and Senior (1967) to be required to minimize the cross section of a sphere loaded by a slot parallel to the incident wave.

The principal effort toward realization of a negative reactance has been in the area of negative impedance converters (NIC's). Considerable success has been achieved in compensating for high-frequency effects and extending the useful range of operation of the NIC into the VHF range. These results are discussed in Section 3.

II

THEORETICAL STUDIES

The principal theoretical problem arising from the study of impedance loading can be broadly formulated in the following terms:

Given the real part, $R(\omega)$, and the imaginary part, $X(\omega)$, of an impedance on some frequency interval, $\omega_1 \leq \omega \leq \omega_2$, what can be said concerning the behavior of these functions outside the band $[\omega_1, \omega_2]$?

A number of more specific questions can be based on this general statement of the problem. For example:

Does there exist a function $Z(p)$, analytic in the right-half p-plane, whose real and imaginary parts are equal to $R(\omega)$ and $X(\omega)$, respectively, for $p = j\omega$, $\omega_1 \leq \omega \leq \omega_2$?

If such a function exists, is it unique ?

Assuming that $Z(p)$ exists, what procedure can be used to find it, at least for $p = j\omega$?

What are the conditions under which $Z(p)$ is positive-real; that is, under what conditions will $\mathrm{Re}\left[Z(j\omega)\right] \geq 0$ for all ω be satisfied ?

All the questions have been considered, some of them by several different methods. All of them have been answered at least in part; $Z(p)$ does exist, it is unique, $Z(j\omega)$ can be found for all ω, and some necessary (though not sufficient) conditions for $Z(p)$ to be positive-real are known.

2.1 General Method of Attack

The most powerful analytic tool in this investigation has been the Hilbert Transform, which relates the real and imaginary parts of a function analytic in the closed right-half plane. If Z (p) is such a function, then

$$\oint_C \frac{Z(p)}{p - j\omega_o}\, dp = 0 \tag{2.1}$$

where C is the contour shown in Fig. 2-1. Letting the radius of the small semicircle approach zero and that of the large semicircle approach infinity, and separating real and imaginary parts, we obtain

$$R(\omega) = -\frac{1}{\pi}\int_{-\infty}^{\infty} \frac{X(\lambda)\, d\lambda}{\lambda - \omega} + R(\infty) \tag{2.2a}$$

$$X(\omega) = \frac{1}{\pi}\int_{-\infty}^{\infty} \frac{R(\lambda)\, d\lambda}{\lambda - \omega} \tag{2.2b}$$

These integrals are improper, and must be evaluated in the Cauchy principal-value sense, that is,

$$\int_{-\infty}^{\infty} d\lambda = \lim_{\epsilon \to 0}\left[\int_{-\infty}^{\omega-\epsilon} d\lambda + \int_{\omega+\epsilon}^{\infty} d\lambda\right] . \tag{2.3}$$

The basic Hilbert Transform pair, (2.2a) and (2.2b), may be manipulated into a number of other useful forms. In particular, if the integrals are expressed as the sum of two integrals, one from $-\infty$ to 0 and the other from 0 to ∞, one obtains, after a suitable change of variable

$$R(\omega) = -\frac{2}{\pi}\int_{0}^{\infty} \frac{\lambda X(\lambda)\, d\lambda}{\lambda^2 - \omega^2} + R(\infty) \tag{2.4a}$$

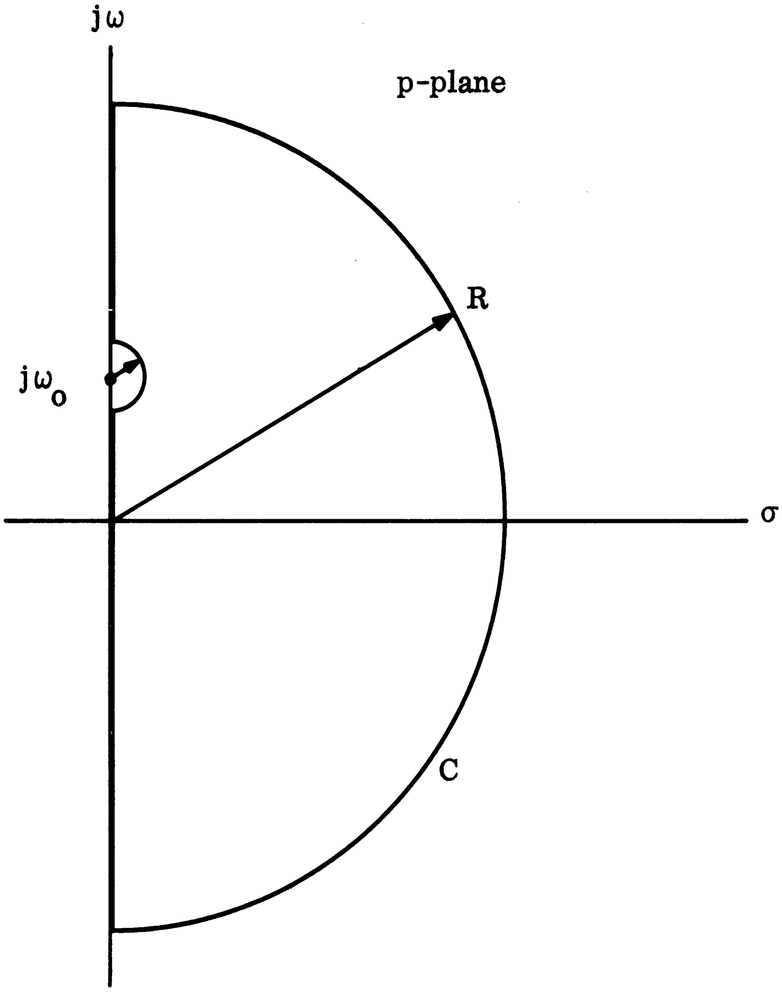

FIG. 2-1: CONTOUR OF INTEGRATION FOR HILBERT TRANSFORMS.

$$X(\omega) = \frac{2\omega}{\pi} \int_0^\infty \frac{R(\lambda)\, d\lambda}{\lambda^2 - \omega^2} \tag{2.4b}$$

where use has been made of the fact that $R(\omega)$ is an even function and $X(\omega)$ an odd function.

The Hilbert Transform need not be applied directly to $Z(p)$. An especially useful set of relations is obtained by applying the transform to the function $Z(p) \big/ \sqrt{1+p^2}$. Of the four equations thus obtained, the two of greatest value in this work are

$$R(\omega) = \frac{2}{\pi} \sqrt{1-\omega^2} \left[-\int_0^1 \frac{\lambda X(\lambda)\, d\lambda}{(\lambda^2-\omega^2)\sqrt{1-\lambda^2}} + \int_1^\infty \frac{\lambda R(\lambda)\, d\lambda}{(\lambda^2-\omega^2)\sqrt{\lambda^2-1}} \right], \quad 0 < \omega < 1 \tag{2.5a}$$

$$X(\omega) = \frac{2\omega}{\pi} \sqrt{1-\omega^2} \left[\int_0^1 \frac{R(\lambda)\, d\lambda}{(\lambda^2-\omega^2)\sqrt{1-\lambda^2}} + \int_1^\infty \frac{X(\lambda)\, d\lambda}{(\lambda^2-\omega^2)\sqrt{\lambda^2-1}} \right], \quad 0 < \omega < 1. \tag{2.5b}$$

A simplification which has been used in much of this investigation is that of assuming $R(\omega)$ and $X(\omega)$ known in the band $0 < \omega < 1$ rather than for $\omega_1 < \omega < \omega_2$. This assumption results in considerable simplification of the mathematical manipulations without any significant loss of generality, since the results obtained for the "low-pass" case can be readily extended to the "band-pass" case

The fundamental problem of this investigation has been the solution of the integral equations, (2.5a) and (2.5b), for the unknown parts of $R(\omega)$ and $X(\omega)$. Although closed forms of solution have not been found, a number of numerical techniques have been developed; these are discussed in succeeding sections of this report.

2.2 Bounds on Function Behavior

It is reasonable to ask what restrictions are placed on $R(\omega)$ and $X(\omega)$ in $(0, 1)$ under the assumption, necessary for physical realizability of a passive network, that $R(\omega)$ be non-negative for all ω. From (2.4b)

$$X(\omega) = \frac{2\omega}{\pi} \int_0^1 \frac{R(\lambda)\, d\lambda}{\lambda^2 - \omega^2} + \frac{2\omega}{\pi} \int_1^\infty \frac{R(\lambda)\, d\lambda}{\lambda^2 - \omega^2} . \tag{2.6}$$

With $R(\omega) \geq 0$, the second integral in (2.6) is a non-negative, non-decreasing function of ω for $0 < \omega < 1$. Therefore

$$X(\omega) \geq \frac{2\omega}{\pi} \int_0^1 \frac{R(\lambda)\, d\lambda}{\lambda^2 - \omega^2} , \quad 0 < \omega < 1 \tag{2.7}$$

$$\frac{dX(\omega)}{d\omega} \geq \frac{d}{d\omega} \left[\frac{2\omega}{\pi} \int_0^1 \frac{R(\lambda)\, d\lambda}{\lambda^2 - \omega^2} \right] , \quad 0 < \omega < 1 . \tag{2.8}$$

By adding and subtracting $R(\omega)$ inside the integral we get

$$\frac{2\omega}{\pi} \int_0^1 \frac{R(\lambda)\, d\lambda}{\lambda^2 - \omega^2} = \frac{2\omega}{\pi} \int_0^1 \frac{R(\lambda) - R(\omega)}{\lambda^2 - \omega^2} + \frac{1}{\pi} R(\omega) \ln \left(\frac{1 - \omega}{1 + \omega} \right) \tag{2.9}$$

where the first integral on the right is now proper. This result indicates that the bounds of (2.7) and (2.8) are rather weak, since the function on the right has a logarithmic singularity, approaching $-\infty$ as $\omega \rightarrow 1-$. For example, for

$$R(\omega) = \frac{1}{1+\omega^2} , \quad X(\omega) = \frac{-\omega}{1+\omega^2} , \quad 0 < \omega < 1 \tag{2.10}$$

we have

$$-\frac{\omega}{1+\omega^2} \geq -\frac{\omega}{1+\omega^2}\left[\frac{1}{2}+\frac{1}{\pi\omega}\,\ell n\left(\frac{1+\omega}{1-\omega}\right)\right] \tag{2.11}$$

and also that the slope of the left-hand term of (2.11) must exceed that of the right-hand term. These two functions are plotted in Fig. 2-2, which shows the weakness of the inequality near $\omega = 1$.

It should be pointed out that inequalities (2.7) and (2.8) become much stronger if $R(1) = 0$, but of course this is a special case.

A stronger inequality can be obtained by observing that the second integral on the right side of (2.5a) is non-negative for $0 < \omega < 1$. Thus we have

$$R(\omega) \geq -\frac{2}{\pi}\sqrt{1-\omega^2}\int_0^1 \frac{\lambda X(\lambda)\,d\lambda}{(\lambda^2-\omega^2)\sqrt{1-\lambda^2}}\,, \quad 0 < \omega < 1 \tag{2.12}$$

or more generally

$$R(\omega) \geq -\frac{2}{\pi}\sqrt{\omega_o^2-\omega^2}\int_0^{\omega_o} \frac{\lambda X(\lambda)\,d\lambda}{(\lambda^2-\omega^2)\sqrt{\omega_o^2-\lambda^2}}\,, \quad 0 < \omega < \omega_o \tag{2.13}$$

Using the same pair of functions as the previous example;

$$R(\omega) = \frac{1}{1+\omega^2}\,, \qquad X(\omega) = -\frac{\omega}{1+\omega^2} \tag{2.14}$$

the inequality (2.13) is shown in Fig. 2-3 for $\omega_o = \frac{1}{2}$, $\omega_o = 1$, and $\omega_o = 2$. It will be noted that as ω_o increases, the lower bound approaches the function itself, as one would expect. Letting $\omega_o \longrightarrow \infty$ in (2.13) and comparing with (2.4a), we

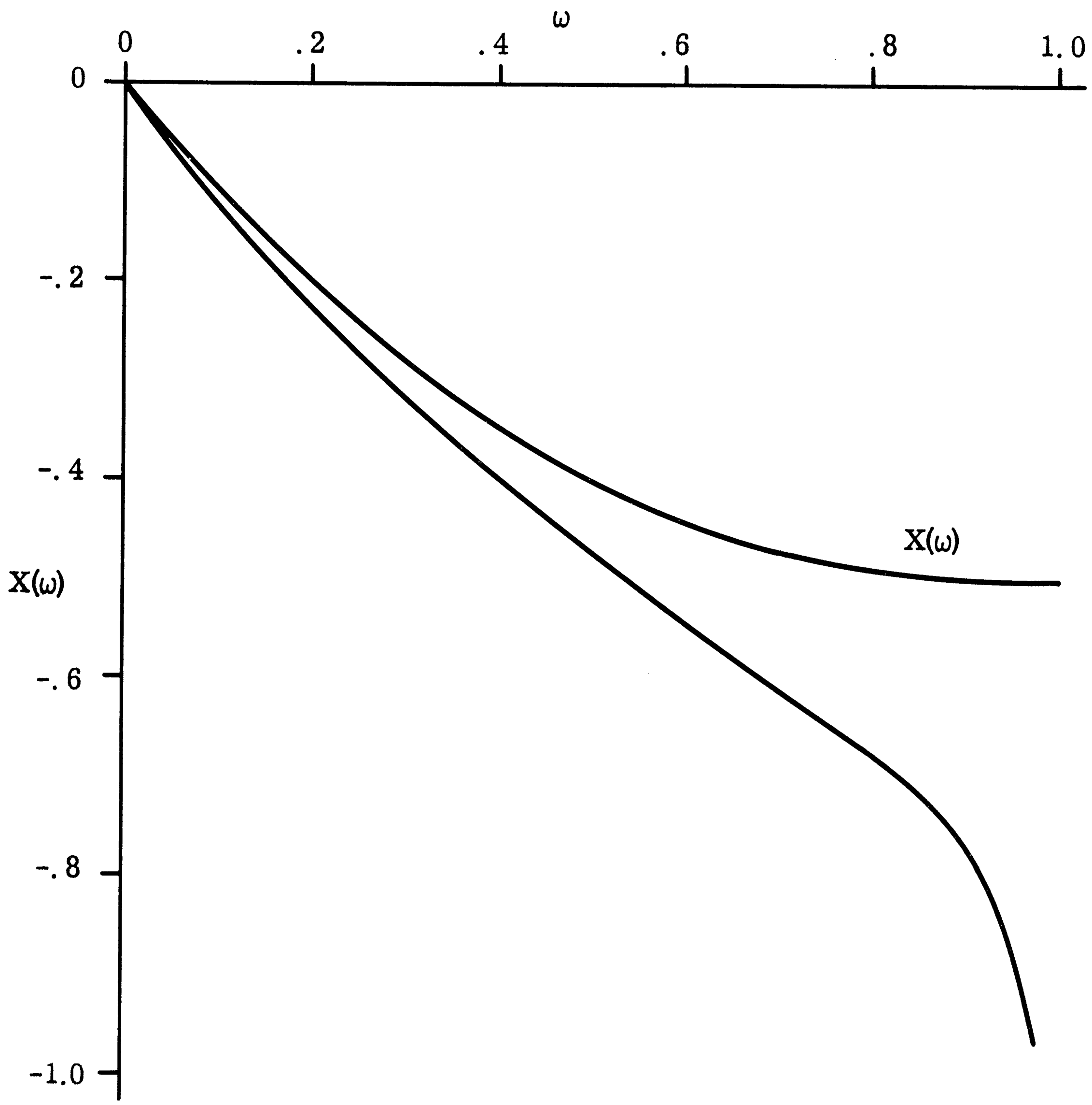

FIG. 2-2: LOWER BOUND ON X(ω).

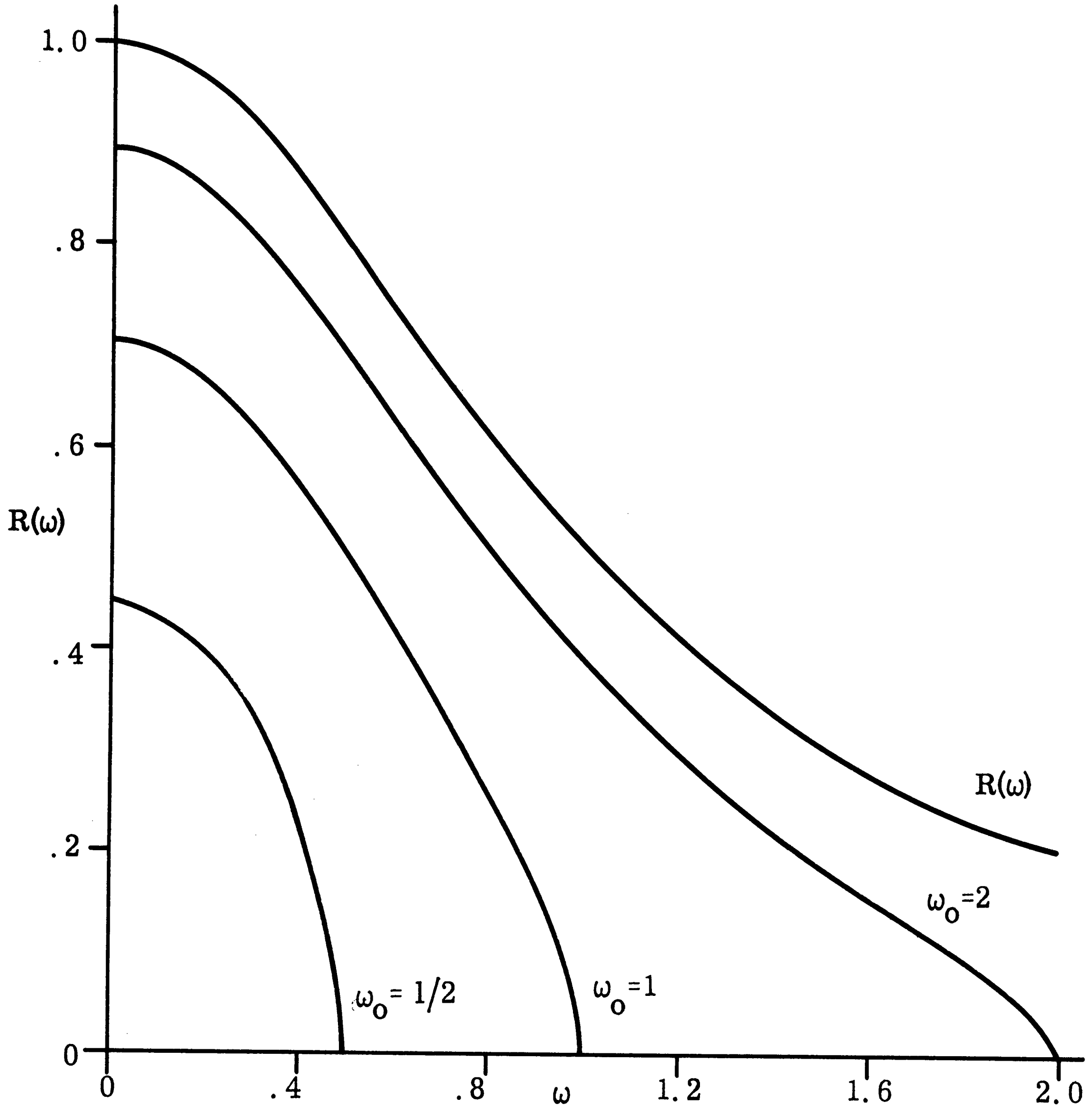

FIG. 2-3: LOWER BOUNDS ON R(ω).

see that the lower bound actually approaches $R(\omega) - R(\infty)$; this makes no difference in the example or indeed in most cases of practical interest.

If the right side of (2.13) goes negative anywhere on $(0, \omega_o)$ (indicating that $R(\infty)$ is non-zero), a better lower bound can be obtained by adding a suitable constant to make the minimum value of the lower bound zero.

2.3 Fourier Methods

One way of approaching the problem of finding $R(\omega)$ and $X(\omega)$ outside the band in which they are given is by means of the change of variable

$$\omega = \frac{1-p}{1+p} \tag{2.15}$$

which maps the right-half p-plane into the unit disc in the ω-plane. If $Z(p)$ is analytic for $\mathrm{Re}(p) \geq 0$, then $Z(\omega)$ will be analytic for $|\omega| \leq 1$. Thus, a power series expansion around the origin

$$Z(\omega) = A_o + A_1\omega + A_2\omega^2 + \ldots \tag{2.16}$$

converges for $|\omega| \leq 1$. On the unit circle, let

$$\omega = \epsilon^{-j\phi} \quad . \tag{2.17}$$

Then

$$\begin{aligned} Z(\epsilon^{-j\phi}) &= A_o + A_1\epsilon^{-j\phi} + A_2\epsilon^{-2j\phi} + \ldots \\ &= (A_o + A_1\cos\phi + A_2\cos 2\phi + \ldots) \\ &\qquad - j(A_1\sin\phi + A_2\sin 2\phi + \ldots) \quad . \end{aligned} \tag{2.18}$$

From (2.15) and (2.17) we have

$$\omega = \tan \frac{\phi}{2} \quad , \qquad -\pi < \phi < \pi \tag{2.19}$$

so that

$$R^*(\phi) = R(\tan \frac{\phi}{2}) = A_o + A_1 \cos\phi + A_2 \cos 2\phi + \ldots \tag{2.20}$$

$$X^*(\phi) = X(\tan \frac{\phi}{2}) = B_1 \sin\phi + B_2 \sin 2\phi + \ldots$$

$$= -A_1 \sin\phi - A_2 \sin 2\phi + \ldots \tag{2.21}$$

We thus have the Wiener-Lee criterion for physical realizability

$$A_n + B_n = 0 \quad , \quad n = 1, 2, \ldots \; . \tag{2.22}$$

If $R(\omega)$ and $X(\omega)$ are given for $\omega \epsilon (0, 1)$, then $R^*(\phi)$ and $X^*(\phi)$ are known for $-\frac{\pi}{2} < \phi < \frac{\pi}{2}$. (The extension to negative values of ϕ comes from the fact that R and X are respectively even and odd.) One possible method of solution is to find a Fourier Series which gives the best fit (in the least-square sense) to $R^*(\phi)$ and $X^*(\phi)$, subject to the constraint (2.22). This method was used by Redheffer (1947); unfortunately, the equations are rather difficult to generate, and the determination of R^* and X^* for $|\phi| > \frac{\pi}{2}$ requires the summation of a Fourier Series.

The present investigation made use of a different approach. Assume that the range $\frac{\pi}{2} < \phi < \pi$ is divided into n equal intervals, and that $R^*(\phi)$ and $X^*(\phi)$ in each of these intervals may be approximated by a constant. Thus we have

$$\left.\begin{array}{l} R^*(\phi) = R_k \\ X^*(\phi) = X_k \end{array}\right\} , \quad \phi_{k-1} < \phi < \phi_k \; , \tag{2.23}$$

where

$$\phi_k = \frac{\pi}{2} + k\frac{\pi}{2n} \quad . \tag{2.24}$$

The Fourier coefficients are then given by

$$A_m = \frac{2}{\pi}\left\{\int_0^{\pi/2} R^*(\phi)\cos m\phi \, d\phi + \sum_{k=1}^{n} \int_{\phi_{k-1}}^{\phi_k} R_k \cos m\phi \, d\phi \right\} \tag{2.25}$$

$$B_m = \frac{2}{\pi}\left\{\int_0^{\pi/2} X^*(\phi)\sin m\phi \, d\phi + \sum_{k=1}^{n} \int_{\phi_{k-1}}^{\phi_k} X_k \sin m\phi \, d\phi \right\}. \tag{2.26}$$

Applying the Wiener - Lee criterion we obtain, after evaluating the right-hand integrals in (2.25) and (2.26)

$$- \int_0^{\pi/2} \left(R^*(\phi)\cos m\phi + X^*(\phi)\sin m\phi\right) d\phi =$$

$$= \sum_{k=1}^{n} \left\{ R_k \frac{\sin m\phi_k - \sin m\phi_{k-1}}{m} - X_k \frac{\cos m\phi_k - \cos m\phi_{k-1}}{m} \right\}. \tag{2.27}$$

For $m = 1, 2, \ldots, 2n$, (2.27) yields a set of $2n$ simultaneous linear equations for the $2n$ unknowns $R_1, \ldots, R_n, X_1, \ldots, X_n$. The coefficient matrix is independent of R^* and X^*, although it depends on n.

Aside from the approximate nature of the solution, this method has the disadvantage that $R(\omega)$ and $X(\omega)$ are found as the real and imaginary parts of an impedance whose behavior is restricted. From (2.15) and (2.16) we have

$$Z(p) \approx A_o + A_1 \left(\frac{1-p}{1+p}\right) + \ldots + A_n \left(\frac{1-p}{1+p}\right)^n =$$

$$= \frac{a_o + a_1 p + \ldots + a_n p^n}{(1+p)^n} \quad . \tag{2.28}$$

Since all the poles of $Z(p)$ are at $p = -1$, $Z(p)$ lacks the approximating power of a general, nth order function.

The computational difficulties of this method are avoided by using an alternative Fourier method discussed in the next section.

2.4 Alternative Fourier Method

Equations (2.5a) and (2.5b) may be written in the form

$$f(\omega) = \frac{\pi R(\omega)}{2\sqrt{1-\omega^2}} + \int_0^1 \frac{\lambda X(\lambda)\, d\lambda}{(\lambda^2-\omega^2)\sqrt{1-\lambda^2}} = \int_1^\infty \frac{\lambda R(\lambda)\, d\lambda}{(\lambda^2-\omega^2)\sqrt{\lambda^2-1}} \, , \quad 0 \leq \omega \leq 1 \tag{2.29a}$$

$$g(\omega) = \frac{\pi X(\omega)}{2\omega\sqrt{1-\omega^2}} - \int_0^1 \frac{R(\lambda)\, d\lambda}{(\lambda^2-\omega^2)\sqrt{1-\lambda^2}} = \int_1^\infty \frac{X(\lambda)\, d\lambda}{(\lambda^2-\omega^2)\sqrt{\lambda^2-1}} \, , \quad 0 \leq \omega \leq 1 \tag{2.29b}$$

where $f(\omega)$ and $g(\omega)$ are known functions for $0 \leq \omega \leq 1$.

Since $X(\lambda)$ is an odd function, it may be written as $\lambda E(\lambda)$, where $E(\lambda)$ is even. This substitution makes the right-hand sides of (2.29a) and (2.29b) formally identical, so that it will suffice to consider only one of them.

Making the change of variable

$$\lambda = \sec\theta \tag{2.30}$$

in (2.29a) we have

$$f(\omega) = \int_0^{\pi/2} \frac{R^*(\theta)\,d\theta}{1-\omega^2\cos^2\theta} \quad , \tag{2.31}$$

where

$$R^*(\theta) = R(\sec\theta) \quad . \tag{2.32}$$

Note that if $R^*(\theta) \geq 0$ for $0 < \theta < \pi/2$, the right-hand side of (2.31), and all its partial derivatives with respect to ω, are non-negative for $0 \leq \omega < 1$. Therefore, if $f(\omega)$ is expanded in a power series about the origin

$$f(\omega) = \sum_{n=0}^{\infty} K_n\,\omega^{2n} \tag{2.33}$$

the K_n's must all be non-negative.

The term $(1-\omega^2\cos^2\theta)^{-1}$ appearing on the right side of (2.31) may be expanded by the binomial theorem into an infinite series which converges absolutely for $\omega < 1$. Thus we have

$$f(\omega) = \sum_{n=0}^{\infty} K_n\,\omega^{2n} = \int_0^{\pi/2} R^*(\theta)\sum_{n=0}^{\infty} \omega^{2n}\cos^{2n}\theta\,d\theta \quad . \tag{2.34}$$

Since the series converges absolutely, we may interchange the order of integration and summation and equate coefficients of like powers, obtaining

$$K_n = \int_0^{\pi/2} R^*(\theta) \cos^{2n} \theta \, d\theta \quad . \tag{2.35}$$

Since

$$\cos^{2(n+1)} \theta < \cos^{2n} \theta \quad , \quad 0 < \theta < \frac{\pi}{2} \quad , \tag{2.36}$$

it follows that if $R^*(\theta) > 0$ for $0 < \theta < \pi/2$, then

$$K_n > K_{n+1} > 0, \quad \text{all } n \quad . \tag{2.37}$$

This inequality is a necessary (but by no means sufficient) condition for the existence of a pair of functions $R(\omega)$ and $X(\omega)$, satisfying Eqs. (2.29a) and (2.29b), with $R(\omega) \geq 0$ for all ω. Such a pair of functions we will call "compatible".

The necessary conditions for compatibility may be summarized by the relations

$$\frac{\partial^n f(\omega)}{\partial (\omega^2)^n} \geq 0 \;, \qquad n = 0, 1, 2, \ldots . \qquad 0 \leq \omega < 1 \tag{2.38}$$

$$(n+1) \left. \frac{\partial^n f(\omega)}{\partial (\omega^2)^n} \right|_{\omega = 0} > \left. \frac{\partial^{n+1} f(\omega)}{\partial (\omega^2)^{(n+1)}} \right|_{\omega = 0} > 0, \quad \text{all } n \; . \tag{2.39}$$

In order to solve for the unknown part of $R(\omega)$, we make the further change of variable $\theta = \phi/2$ in (2.35), obtaining

$$K_n = \frac{1}{2} \int_0^{\pi} R'(\phi) \cos^{2n} \frac{\phi}{2} \, d\phi \tag{2.40}$$

where

$$R'(\phi) = R\left(\sec\frac{\phi}{2}\right) \quad . \tag{2.41}$$

Since $R'(\phi)$ is an even function it can be expanded in a Fourier cosine series

$$R'(\phi) = \sum_{m=0}^{\infty} A_m \cos m\phi \quad . \tag{2.42}$$

Making use of the trigonometric identity

$$\cos^{2n}\frac{\phi}{2} = \frac{1}{2^{2n}}\left\{\sum_{j=0}^{n-1} 2\binom{2n}{j}\cos(n-j)\phi + \binom{2n}{n}\right\} \tag{2.43}$$

and substituting (2.42) and (2.43) into (2.40) we obtain

$$K_n = \frac{1}{2^{2n+1}}\int_0^{\pi}\sum_{m=0}^{\infty} A_m \cos m\phi\left\{\sum_{j=0}^{n-1} 2\binom{2n}{j}\cos(n-j)\phi + \binom{2n}{n}\right\}d\phi \quad . \tag{2.44}$$

From the orthogonality relation

$$\int_0^{\pi}\cos m\phi\cos(n-j)\phi\, d\phi = \begin{cases}\pi\ , & m = n-j = 0\\ \frac{\pi}{2}\ , & m = n-j \neq 0\\ 0\ , & m \neq n-j\end{cases} \tag{2.45}$$

we obtain finally

$$K_n = \frac{\pi}{2^{2n+1}}\sum_{j=0}^{n} A_{n-j}\binom{2n}{j} \quad . \tag{2.46}$$

This relation is solved recursively to obtain

$$A_n = \frac{2^{2n+1}}{\pi} K_n - \sum_{j=1}^{n} A_{(n-j)} \binom{2n}{j} \quad . \tag{2.47}$$

It would appear that by making use of the relation

$$\cos n\phi = \sum_{k=0}^{n} b_{nk} \cos^{2k} \frac{\phi}{2} \tag{2.48}$$

where

$$b_{nn} = 2^{2n-1} \quad , \tag{2.49}$$

$$b_{nk} = (-1)^{n-k} \frac{2n}{n-k} \binom{n+k-1}{n-k-1} 2^{2k-1} \quad , \; k \neq n \quad , \tag{2.50}$$

in (2.42), one could obtain an expression of the form

$$R'(\phi) = \sum_{k=0}^{\infty} B_k \cos^{2k} \frac{\phi}{2} \tag{2.51}$$

which corresponds to

$$R(\omega) = \sum_{k=0}^{\infty} B_k / \omega^{2k} \quad . \tag{2.52}$$

However, such a form, since it is a power-series expansion about infinity, will be meaningful only if $Z(p)$ has no singularities outside the unit circle. Even for cases satisfying this condition, serious convergence difficulties were encountered, most probably due to the truncation of Eq. (2.42).

This difficulty is easily circumvented by summing the Fourier Series, (2.42), directly, and then changing the abcissa for ϕ to ω by use of the relation

$$\omega = \sec \frac{\phi}{2} . \tag{2.53}$$

Results obtained by applying this technique to known functions have been excellent. The real and imaginary parts of a known impedance, calculated on $(1, \infty)$ using a seven-term series, agreed with the actual values to three significant digits.

The error due to truncation can be estimated rather easily. We note from (2.46) and (2.47) that the relationship between the first $(N+1)$ A_n's and K_n's is independent of the higher-order terms. Thus, truncating the Fourier Series (2.42) at the Nth term is equivalent to truncating the power series (2.34) at the Nth term. A measure of the error is thus given by

$$e(\omega) = f(\omega) - \sum_{n=0}^{N} K_n \omega^{2n} = \sum_{n=N+1}^{\infty} K_n \omega^{2n} , \tag{2.54}$$

where $e(\omega)$ is positive for all ω, since the K_n's are all positive.

To avoid difficulty with singularities, we define

$$F(\omega) = \frac{\pi}{2} R(\omega) + \sqrt{1-\omega^2} \int_0^1 \frac{\lambda X(\lambda) \, d\lambda}{(\lambda^2 - \omega^2) \sqrt{1-\lambda^2}} \tag{2.55}$$

and

$$e^*(\omega) = F(\omega) - \sum_{n=0}^{N} K_n \omega^{2n} \sqrt{1-\omega^2} , \tag{2.56}$$

where $e^*(\omega) \geq 0$, $0 \leq \omega \leq 1$.

We now define the error by

$$E = \frac{\int_0^1 e^*(\omega)\, d\omega}{\int_0^1 F(\omega)\, d\omega} \quad . \tag{2.57}$$

Defining

$$I = \int_0^1 F(\omega)\, d\omega \tag{2.58}$$

and carrying out the integration in the numerator of (2.57) we obtain

$$E = 1 - \frac{\frac{\pi}{2} \sum_{n=0}^{N} K_n \frac{(2n-1)(2n-3)\ldots(3)(1)}{(2n+2)(2n)\quad\ldots(4)(2)}}{I} \quad . \tag{2.59}$$

2.5 Direct Computer Solution

A number of attempts were made to obtain a direct solution by means of the computer. Given $R_o(\omega)$ and $X_o(\omega)$ for $\omega \epsilon (\omega_a, \omega_b)$, the objective is to develop a computer program which will determine either the coefficients of a positive-real rational function or the element values of a passive network, such that the real and imaginary parts of the corresponding impedance approximate, in some sense, $R_o(\omega)$ and $X_o(\omega)$.

The most general approach is by way of a positive-real rational function. The method which was used may be summarized by the following steps:

1) As a starting point, pick the coefficients of a rational function, $Z(p)$, of degree n:

$$Z(p) = \frac{a_n p^n + \ldots + a_1 p + a_o}{b_n p^n + \ldots + b_1 p + b_o} \quad . \tag{2.60}$$

The program will reject $Z(p)$ if it is not positive-real.

2) Evaluate the real and imaginary parts of $Z(p)$, $R(\omega_i)$ and $X(\omega_i)$ respectively, at the $m+1$ frequencies ω_i, where

$$\omega_a = \omega_o < \omega_1 < \ldots < \omega_m = \omega_b \tag{2.61}$$

3) Compute the weighted error

$$E = \sum_{i=0}^{m} w_i \left[\left(R(\omega_i) - R_o(\omega_i) \right)^2 + \left(X(\omega_i) - X_o(\omega_i) \right)^2 \right] \tag{2.62}$$

where the w_i's are the weights.

4) Determine the partial derivatives of E with respect to the coefficients $a_o, a_1, \ldots, a_n, b_o, b_1, \ldots, b_n$ of (2.60) and compute the gradient direction in the $(2n+2)$ - dimensional coefficient space.

5) Move in the negative-gradient direction in coefficient space until one of the following happens:

a) The error reaches a minimum. In this case, compute the new gradient and proceed as above.

b) The function ceases to be positive-real. In this case, retreat along the gradient line back to the positive-real region, compute the gradient again, and proceed as above.

6) When a point is reached from which no further progress can be made (the error cannot be reduced further while remaining in the positive-real region) the search terminates and results are printed.

In practice, this procedure was found to be very slow. This seemed to be due to the fact that the boundaries of the positive-real region in the coefficient space are quite irregular, requiring frequent backtracking and gradient computation. In addition, the process of checking the function for positive-real character is quite time consuming. In addition, since the error is a very complicated function of the coefficients, it was felt that local minima would make the process quite dependent on the initial values of the coefficient. This line of investigation was therefore not pursued further.

A simpler, although less general, procedure is to choose a network configuration and adjust the element values. The condition for physical realizability is now much simpler; all the element values must be non-negative. The procedure which was used was a gradient search (steepest descent method) similar to that outlined above. The most significant difference was that the boundary of the region of physical realizability is much more easily defined in the present case. Whenever movement in the negative-gradient direction caused one or more element values to become negative, they were simply set back to zero before the next step was taken. Thus, the search technique was actually a modified gradient search, since the direction of search deviated from the gradient line near the boundaries at the positive - coefficient region.

This "direct synthesis" technique had much better convergence properties than the rational function approximation. The improvement appeared to be due to the simple nature of the constraints in this case (element values non-negative) compared to those of the previous case (function positive-real). A number of difficulties remained, however. The method is obviously dependent on the configuration chosen for the network; a ladder network was used in this study for its computational simplicity, but this may not be the best choice from a practical standpoint. The problem of local minima and dependence on initial values still remained. Further, it became apparent that, due to the high dimensionality of the problem and the extremely nonlinear dependence of the error function on the element values, the gradient search technique was not a sufficiently powerful method.

A quadratic search was then tried. In contrast to the gradient search, which essentially linearizes the function to be minimized, the quadratic search retains another term of the power series expansion. This technique will minimize a quadratic form in a single step. Unfortunately, the problem at hand did not involve a quadratic form but a much more complicated function, to which the method was totally unsuited. In fact, the procedure was unstable, making large jumps in element-value space without getting any closer to the minimum point.

No further effort was devoted to this area of direct computer solution. It was quite obvious that much more powerful search techniques would be required involving much longer computation times. Judging from the results obtained thus far, prospects for success are poor, even with the use of more powerful search techniques.

III
EXPERIMENTAL PROGRAM

Since the theoretical studies discussed above are of rather long-range applicability, an experimental study aimed at more immediate results was conducted in parallel. Efforts were directed toward finding a network realization of the impedance shown in Fig. 3-1. This impedance was determined by Chang and Senior (1967) as the required loading impedance for cross-section reduction of a sphere loaded by a circumferential slot in the plane of incidence.

In the region of interest, near $ka = 1$, the desired impedance can be well approximated by a negative reactance, which suggests realization by an active network. Unfortunately, there exists no really coherent theory for the realization of active driving-point impedances; the task was therefore one of choosing from a number of available alternatives those which seemed to have the greatest probability of success in a reasonably short time.

3.1 Tunnel-Diode Network

Because of its size and simplicity, the tunnel diode appeared to be a likely choice for an active element. Properly biased, the tunnel diode may be modelled by a negative resistance in parallel with a capacitance, as shown in Fig. 3-2. The network in which it is embedded was designed on an intuitive basis; essentially, the inductance L paralleling the diode gives a pair of poles in the right-half plane, the RLC combination gives a mirror-image pair in the left-half plane, and L_o moves the poles on to the $j\omega$-axis.

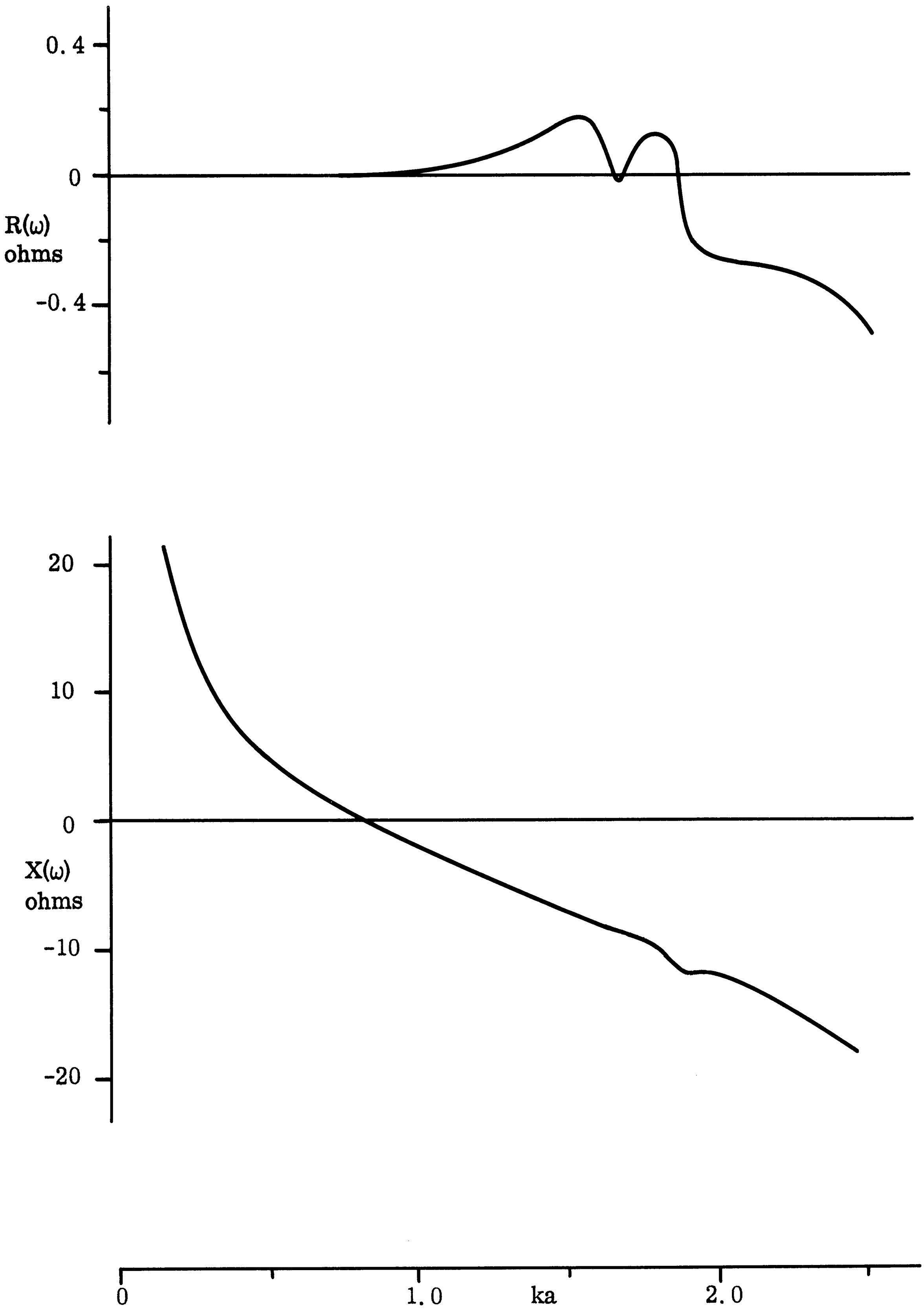

FIG. 3-1: IMPEDANCE TO BE REALIZED.

Straightforward network analysis yields

$$Z = \left(\frac{2}{C}\right) \frac{p\left(p^2 + \frac{1}{LC}\right)}{p^4 + p^2\left(2\,\frac{L_o + L}{L_o L C} - \frac{1}{R^2 C^2}\right) + \frac{L_o + 2L}{L_o L^2 C^2}} \quad . \tag{3.1}$$

If L_o is chosen to satisfy

$$\frac{1}{L_o C} = \frac{1}{2R^2 C^2} + \frac{1}{RC\sqrt{LC}} \tag{3.2}$$

then (3.1) becomes

$$Z = \left(\frac{2}{C}\right) \frac{p\left(p^2 + \frac{1}{LC}\right)}{\left(p^2 + \frac{1}{LC} + \frac{2}{RC\sqrt{LC}}\right)^2} \quad . \tag{3.3}$$

For $p = j\omega$, Z is a pure reactance:

$$Z(j\omega) = jX(\omega) = j\left(\frac{2}{C}\right) \frac{\omega(\omega_a^2 - \omega^2)}{(\omega_b^2 - \omega^2)^2} \tag{3.4}$$

where

$$\omega_a < \omega_b \quad . \tag{3.5}$$

Obviously, $X(\omega)$ is positive for $0 < \omega < \omega_a$ and negative for $\omega_a < \omega < \omega_b$, and thus has negative slope in some region around ω_a; this is the desired type of behavior.

The circuit of Fig. 3-2 was constructed and tested. The predicted frequency response was not observed; the frequency response being essentially that of a passive network. It is felt that this was due to second-order effects, most importantly lead inductance, which were not included in the model of the tunnel diode. Further effort did not appear justified, and the circuit was abandoned.

3.2 Negative Impedance Converter Development

Another likely active element for synthesis is the Negative Impedance Converter (NIC). Its use is readily suggested by the negative-reactance characteristic desired in the present application; in addition, a number of active-synthesis techniques using the NIC have appeared in the literature.

The NIC is a two-port, active network with the property that its input impedance is the negative of its load impedance. Any linear two-port, active or passive, may be characterized by its hybrid parameters:

$$V_1 = h_{11} I_1 + h_{12} V_2 \tag{3.6}$$

$$I_2 = h_{21} I_1 + h_{22} V_2 \quad . \tag{3.7}$$

If the two-port is terminated at port 2 by an impedance Z_L, then the input impedance at port 1 is given by

$$Z_{in} = h_{11} - \frac{h_{12} h_{21}}{h_{22} + Y_L} \quad . \tag{3.8}$$

If $h_{11} = h_{22} = 0$, and if $h_{12} h_{21} = 1$, then

$$Z_{in} = -\frac{1}{Y_L} = -Z_L \tag{3.9}$$

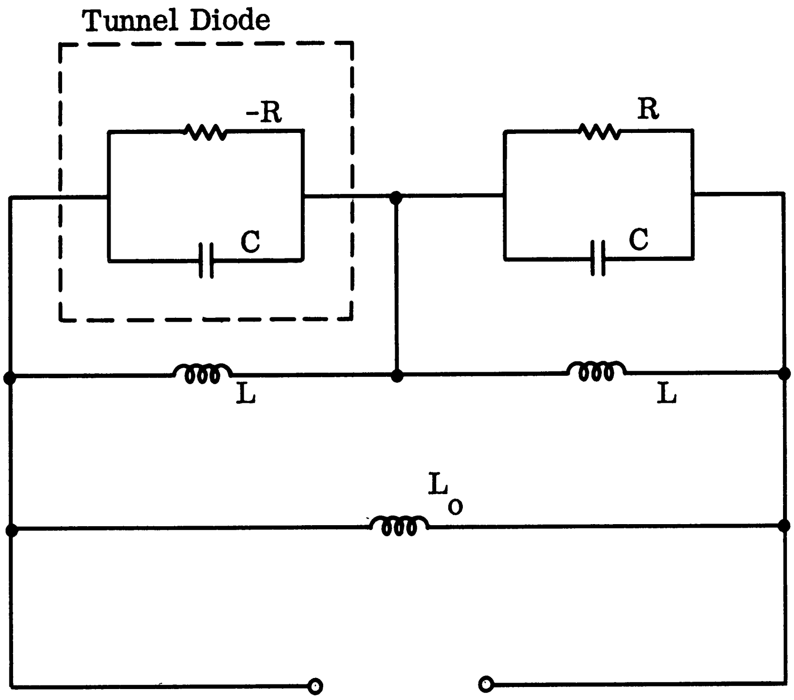

FIG. 3-2: TUNNEL DIODE NETWORK .

which is the desired behavior. In practice, the condition $h_{12} h_{21} = 1$ has been satisfied by one or the other of the alternatives

$$h_{12} = h_{21} = \pm 1 \quad . \tag{3.10}$$

If $h_{12} = h_{21} = 1$, then $V_2 = V_1$ and the device is known as a current inversion NIC, or INIC; if $h_{12} = h_{21} = -1$, the device is a voltage inversion NIC, or VNIC. Most of the circuits appearing in recent literature have been INIC's, and our work has been entirely with this type.

Of the various NIC circuits available, one due to Yanagisawa (1957) was chosen for study. An idealized version of the circuit is shown in Fig. 3-3. It is rather easily shown that, for this circuit

$$V_1 = V_2 \quad , \tag{3.11}$$

$$\frac{I_1}{I_2} = \frac{K Z_1}{(K+1) Z_2 + Z_1} \quad . \tag{3.12}$$

Thus, for large K,

$$\frac{I_1}{I_2} \approx \frac{Z_1}{Z_2} \quad . \tag{3.12}$$

Yanagisawa's realization of this idealized circuit is given in Fig. 3-4a, with the small-signal equivalent circuit in Fig. 3-4b; the similarity between this and the idealized circuit of Fig. 3-3 is quite apparent.

The most important factor limiting the high-frequency performance of this circuit is the collector-base capacitances of the two transistors. In order to have a basis for developing techniques of compensating for these capacitances, the

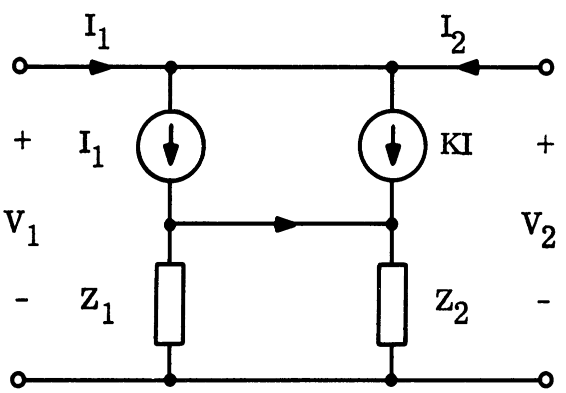

FIG. 3-3: IDEALIZED NEGATIVE IMPEDANCE CONVERTER.

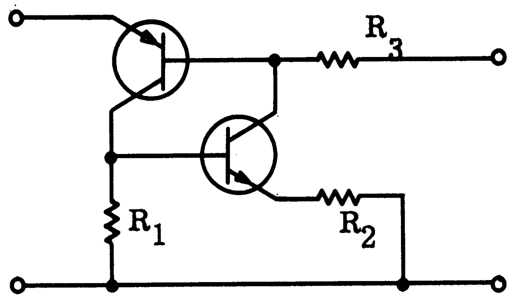

FIG. 3-4a: NEGATIVE IMPEDANCE CONVERTER

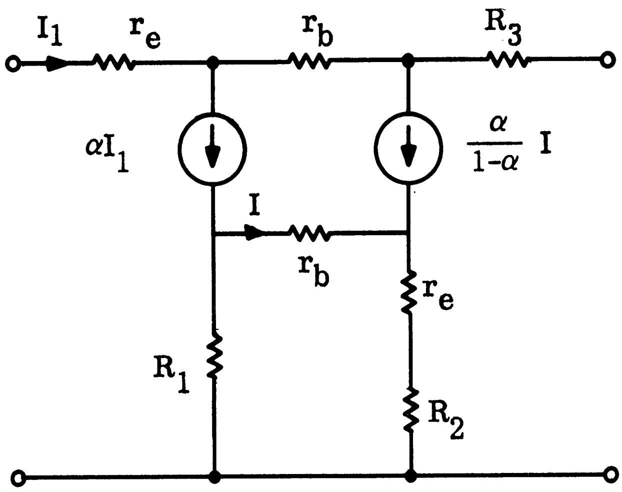

FIG. 3-4b: AC EQUIVALENT CIRCUIT.

simplified equivalent circuit of Fig. 3-5 was used. Base and emitter resistances have been neglected, but the two capacitances have been accounted for by the addition of the capacitance $C = 2C_{cb}$.

A fairly straightforward analysis of this network yields the hybrid parameters:

$$h_{11} = 0 , \qquad h_{12} = 1 ,$$

$$h_{21} = \left(\frac{R_1}{R_2}\right) \frac{1 - pCR_2}{1 + pCR_1} , \qquad h_{22} = pC \, \frac{1 + \frac{R_1}{R_2}}{1 + pCR_1} , \tag{3.14}$$

where α has been assumed to be unity.

Comparing these parameters with the parameters of an ideal NIC, it will be seen that the phase shift in h_{21} is the limiting factor in high-frequency operation; at sufficiently high frequencies, h_{21} approaches a negative real number.

If a capacitance C_2 is placed in parallel with R_2, which is equivalent to the substitution

$$R_2 \longrightarrow \frac{R_2}{1 + pC_2R_2} , \tag{3.15}$$

the h-parameters now become

$$h_{11} = 0 , \qquad h_{12} = 1 ,$$

$$h_{21} = \left(\frac{R_1}{R_2}\right) \frac{1 + p(C_2 - C)R_2}{1 + pCR_1}, \qquad h_{22} = pC \, \frac{1 + \frac{R_1}{R_2} + pC_2R_1}{1 + pCR_1} . \tag{3.16}$$

Now setting $R_1 = R_2$ and $C_2 = 2C$, we have

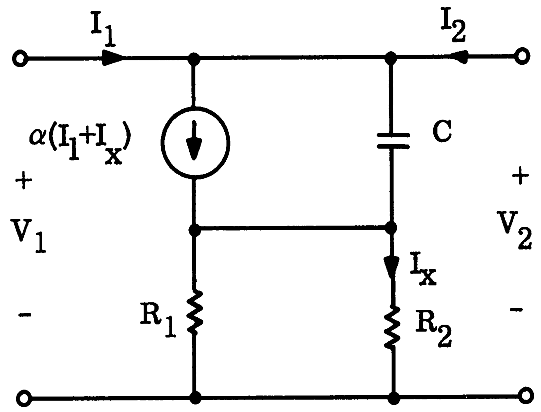

FIG. 3-5: SIMPLIFIED HIGH-FREQUENCY MODEL OF NIC.

$$h_{11} = 0 \ , \qquad h_{12} = 1 \ ,$$

$$h_{21} = 1 \ , \qquad h_{22} = 2pC \ . \tag{3.17}$$

The only departure from ideal behavior now is the non-zero value of h_{22}; this can either be absorbed in the load or compensated for by a capacitance $2pC$ in parallel with the input.

The final version of the circuit is given in Fig. 3-6. Resistors R_3 and R_4 are bias resistors; since at signal frequencies they appear in shunt across the input and output respectively, their effect is cancelled out by the NIC action.

When this circuit was constructed, some difficulties of stability and reliability of operation were encountered, but these were eventually overcome. The bias resistors must be adjusted to prevent "lock-up" (both transistors cut off), but the adjustment is not critical. Oscillation is possible for certain combinations of load impedance and generator impedance (impedance seen looking to the left and the input). For most measurements, it is necessary to pad the input with a resistance in order to prevent oscillation.

Figure 3-7 shows the input impedance of the NIC over the frequency range 1 - 5 MHz. The load impedance was a 270 Ω resistor; a 680Ω resistor was placed in series with the input during measurement to maintain stability, but its resistance has been subtracted from the measured values so that Fig. 3-7 gives the actual input impedance at the NIC terminals.

The fact that the negative resistance seen at the input is on the order of -600 Ω rather than -270Ω is of no consequence, since this is merely a scale factor which can easily be accommodated by changing the load.

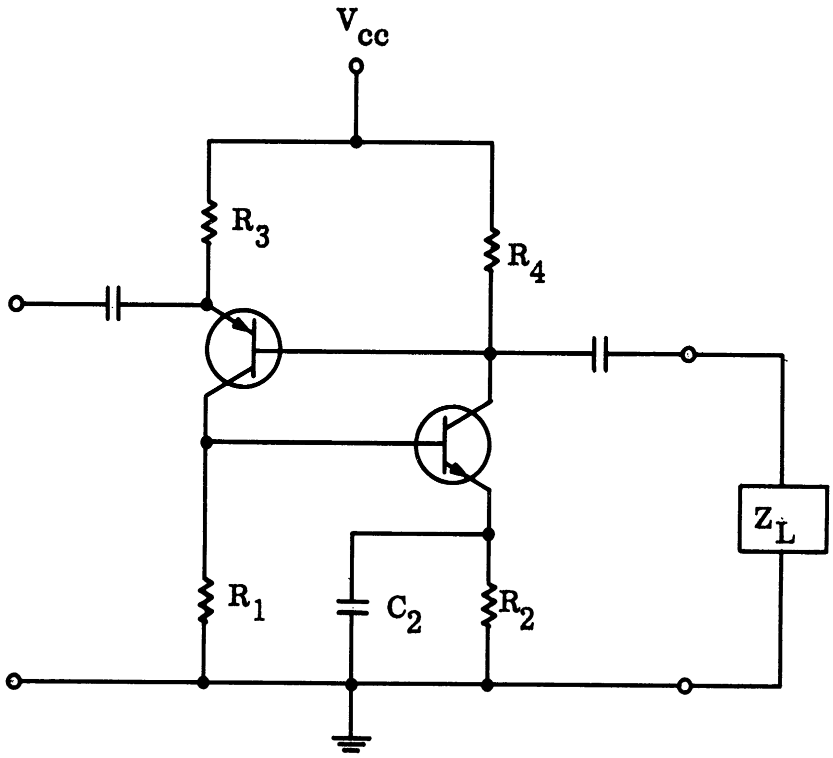

FIG. 3-6: COMPENSATED NIC.

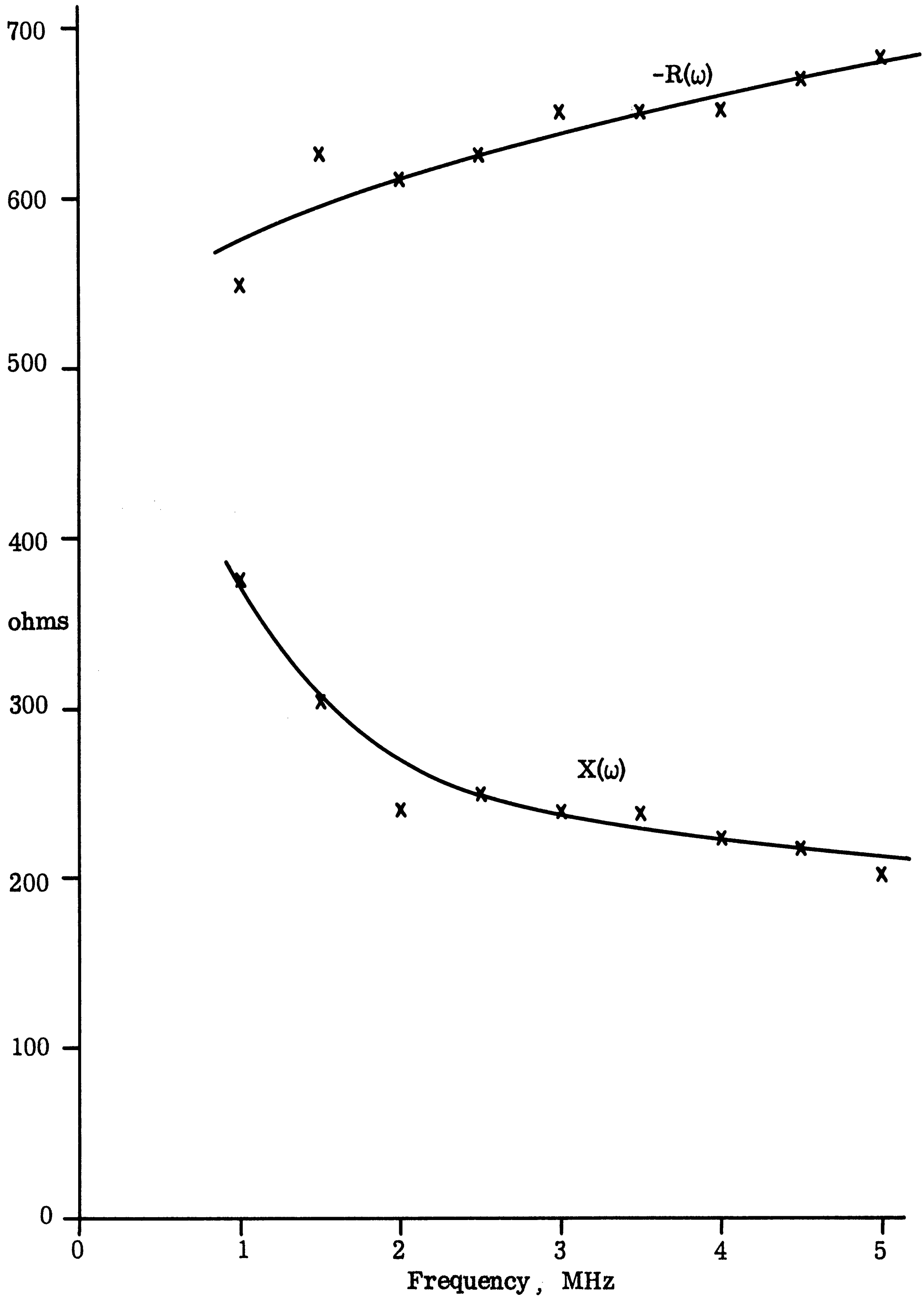

FIG. 3-7: INPUT IMPEDANCE OF NIC; Z_L = 270+j0. (x's indicate measured values; the lines are merely to guide the eye.)

The rather large reactive component of the input impedance is a rather more serious problem, it indicates that the ratio of input impedance to load impedance is complex rather than negative-real. However, the circuit is still in the early stages of development, and considerable improvement can be expected as the development continues. Furthermore, the NIC need not be perfect in order to be useful; this point is discussed in more detail below.

Measurements have thus far been restricted to the 1 - 5 MHz frequency band. This is sufficiently high for the effect of collector capacitance to be significant and low enough that the frequency variation of α may be neglected, and is thus an ideal range for testing and adjusting the compensation scheme.

Since the NIC is essentially a lowpass device, the problem of increasing the bandwidth and the problem of increasing the maximum operating frequency are essentially the same. The critical assumption in the analysis above is that $\alpha \cong 1$, which implies that operation must be at frequencies well below alpha cut-off. To a certain extent, then, improvement in NIC performance depends on improvement in transistor performance. Given the present rate of development of transistor technology, there are good grounds for optimism in this regard.

There is also the possibility of compensating for the frequency dependence of α by the addition of more passive elements to the circuit. This has not been tried so far, since compensation for collector capacitance is a much more pressing problem in the lower VHF band, but there is no reason to believe that it cannot be done.

Even if perfect compensation cannot be obtained, the device may still be useful if some measure of NIC action takes place. Imperfections in the NIC can be overcome by changes in the load impedance. As a trivial example, suppose that an input impedance of $-1 + j0$ is desired at some particular frequency. Assume further that a load impedance of $1 + j0$ produces an input impedance of $-1 - j1$ rather than the desired value. Provided the NIC is operating linearly, a load impedance

$$Z_L = \frac{-1+j0}{-1-j1} = 0.5 - j0.5$$

should give the desired input impedance.

More generally, the process of obtaining a particular input-impedance characteristic using an imperfect NIC would require determining, as a function of frequency, the load impedance needed to give the desired input impedance, and then finding a passive network realizing (or approximately realizing) the necessary load impedance.

3.3 Conclusions

The most important result of the experimental program has been the development and preliminary evaluation of an NIC with frequency compensation for operation in the VHF region. Since NIC development, as reported in the technical literature, has generally been at frequencies below 100 kHz, the results which have been obtained to date are a significant improvement. The immediate objective of continued development in this area is to obtain usable NIC action at 50 MHz or higher. This objective appears quite attainable.

REFERENCES

Chang, S. and T. B. A. Senior (1967), "Study of the Scattering Behavior of a Sphere with an Arbitrarily Placed Circumferential Slot," The University of Michigan Radiation Laboratory Report 5548-6-T, AFCRL-67-0111, AD 648717.

Redheffer, R. M. (1947), "Design of a Circuit to Approximate a Prescribed Amplitude and Phase," J. Math. Phys., 28 (140-147).

Yanagisawa, T. (1957), "RC Active Networks Using Current-Inversion Type Negative Impedance Converters," IRE Trans. on Circuit Theory, CT-4, (140-144).

Unclassified

Security Classification

DOCUMENT CONTROL DATA - R & D

(Security classification of title, body of abstract and indexing annotation must be entered when the overall report is classified)

1. ORIGINATING ACTIVITY *(Corporate author)* The University of Michigan Radiation Laboratory, Dept. of Electrical Engineering, 201 Catherine Street, Ann Arbor, Michigan 48108	2a. REPORT SECURITY CLASSIFICATION UNCLASSIFIED 2b. GROUP

3. REPORT TITLE

NETWORK THEORY PROBLEMS IN IMPEDANCE LOADING

4. DESCRIPTIVE NOTES *(Type of report and inclusive dates)*

Scientific. Interim.

5. AUTHOR(S) *(First name, middle initial, last name)*

E. Lawrence McMahon
Arthur R. Braun
Raymond S. Kasevich

6. REPORT DATE	7a. TOTAL NO. OF PAGES	7b. NO. OF REFS
January 1968	39	3

8a. CONTRACT OR GRANT NO. AF 19(628)-2374	9a. ORIGINATOR'S REPORT NUMBER(S) 5548-8-T Scientific Report No. 8
b. Project, Task, Work Unit Nos. 5635-02-01	
c. DoD Element 61445014	9b. OTHER REPORT NO(S) *(Any other numbers that may be assigned this report)* AFCRL-68-0027
d. DoD Subelement 681305	

10. DISTRIBUTION STATEMENT

1 - Distribution of this document is unlimited. It may be released to the Clearinghouse, Department of Commerce, for sale to the general public.

11. SUPPLEMENTARY NOTES	12. SPONSORING MILITARY ACTIVITY
TECH, OTHER	Air Force Cambridge Research Laboratories (CRD) L.G. Hanscom Field Bedford, Massachusetts 01730

13. ABSTRACT

Relationships between the real and imaginary parts of an impedance are studied. Given the real and imaginary parts in a finite frequency band, a technique is developed for finding these parts outside the band. Conditions under which the real port remains positive for all ω are given.

Use of a negative impedance converter for realization of a particular impedance arising from impedance loading studies is discussed. A method of compensating for collector capacitance and extending operation of a transistorized NIC into the VHF region is given.

DD FORM 1 NOV 65 1473

Unclassified

Security Classification

14. KEY WORDS	LINK A		LINK B		LINK C	
	ROLE	WT	ROLE	WT	ROLE	WT
NETWORK THEORY						
HILBERT TRANSFORMS						
INTEGRAL EQUATIONS						
NEGATIVE IMPEDANCE CONVERTERS						
IMPEDANCE LOADING						